The Journal of Veterinary Medical Science

FULL PAPER

Internal Medicine

# Right ventricular systolic and diastolic function assessed by two-dimensional speckle tracking echocardiography in dogs with myxomatous mitral valve disease

**Yunosuke YUCHI[1)], Ryohei SUZUKI[1)]*, Takahiro TESHIMA[1)], Hirotaka MATSUMOTO[1)] and Hidekazu KOYAMA[1)]**

[1)]Laboratory of Veterinary Internal Medicine, School of Veterinary Medicine, Faculty of Veterinary Science, Nippon Veterinary and Life Science University, 1-7-1 Kyonan-cho, Musashino-shi, Tokyo 180-8602, Japan

**ABSTRACT.** Pulmonary hypertension (PH) is a common comorbidity in dogs with myxomatous mitral valve disease (MMVD), and can induce various changes in the right heart, such as right ventricular (RV) hypertrophy, dilatation, and dysfunction. We hypothesized that RV function, not only systolic function but also diastolic function, could be worsened with PH progression. We aimed to compare RV systolic and diastolic function in dogs with MMVD. Twenty healthy dogs and sixty-eight dogs with MMVD were enrolled. Dogs with MMVD were classified into the probability of PH. Two-dimensional and Doppler echocardiographic indices for right heart and two-dimensional speckle tracking echocardiography indices were measured. The morphological indicators of the right heart were significantly higher only in the high probability of PH group. The RV strain, early-diastolic and systolic strain rates were significantly lower in the high probability of PH group than those in the low and intermediate probability of PH groups. Multivariate analysis showed that increased RV internal dimension normalized by body weight and RV myocardial performance index were significantly associated with the presence of right-sided congestive heart failure. Speckle tracking echocardiography-derived RV systolic and diastolic function were activated in the low and intermediate probability of PH groups. However, dogs with high probability of PH showed RV myocardial dysfunction and dilatation. Increased RV myocardial performance index and end-diastolic RV internal dimension normalized by body weight were significantly associated with the presence of right-sided congestive heart failure in dogs with MMVD.

**KEY WORDS:** canine, congestive heart failure, post-capillary pulmonary hypertension, right ventricular myocardial performance index

*J. Vet. Med. Sci.*
83(12): 1918–1927, 2021
doi: 10.1292/jvms.21-0195

Received: 29 March 2021
Accepted: 23 October 2021
Advanced Epub:
4 November 2021

Pulmonary hypertension (PH) is a common comorbidity in dogs with myxomatous mitral valve disease (MMVD), characterized by an increase in the pulmonary artery pressure with or without pulmonary vascular resistance. Particularly, PH secondary to elevated left atrial pressure is hemodynamically classified into post-capillary PH [4, 14, 22]. It can induce various changes in the right heart, such as right ventricular (RV) hypertrophy, dilatation, and dysfunction, which might eventually lead to right-sided congestive heart failure (R-CHF) [12, 46]. Recent study has reported that RV dilatation and systolic dysfunction were associated with worse outcomes in dogs with PH [45]. Additionally, several human studies have reported that RV diastolic dysfunction was also induced by PH through hypertrophy, fibrosis, and stiffening of RV cardiomyocytes [4–6, 27, 29, 41]. Therefore, RV diastolic dysfunction might also be involved in the development of worse outcomes in PH progression.

A right heart catheterization is a gold standard for the assessment of RV function [15, 30]. However, it has limited availability to perform catheterization in dogs due to the need for anesthesia. Therefore, various echocardiographic variables have been tried to use for the disease state evaluation of PH as alternatives to invasive indicators, but the ability of echocardiographic indices to reliably evaluate RV function is limited [4–6, 30, 39, 41, 44]. Recently, two-dimensional speckle tracking echocardiography (2D-STE) could evaluate the regional and entire RV myocardial function and may reflect the intrinsic RV function [2]. Especially, 2D-STE-derived RV strain rate (RV-SrL) could evaluate the RV diastolic function as well as systolic function with the low dependency of angle and cardiac translation, and various human studies have used as the indicators for RV systolic and diastolic function [19, 31, 47].

*Correspondence to: Suzuki, R.: ryoheisuzuki@nvlu.ac.jp

To the best of our knowledge, a few studies have assessed RV systolic function alone, and no known study has assessed the diastolic function in dogs with PH, although PH could induce RV diastolic dysfunction as well. Additionally, certain human study has reported that RV diastolic function might precede systolic dysfunction in patients with PH [27]. We hypothesized that RV function, not only systolic function but also diastolic function, could be worsened with PH progression and that RV diastolic dysfunction might also be associated with the presence of R-CHF. Therefore, this study aimed to assess the relationship between PH probability and echocardiographic indices for right heart function in dogs with post-capillary PH secondary to MMVD.

## MATERIALS AND METHODS

This was a prospective, observational study. Dogs that underwent cardiac screening at a university veterinary medical hospital in Japan were recruited from October 2017 to May 2019. All procedures followed the Guidelines for Institutional Laboratory Animal Care and Use of Nippon Veterinary and Life Science University in Japan, and it was approved by the ethical committee for animal use of the Nippon Veterinary and Life Science University Veterinary Medical Teaching Hospital, Japan (approval number: R2-5). Written informed consent authorizing the participation of the dogs in this study was obtained from all the dogs' owners. All echocardiographic examinations were performed by a single investigator. All echocardiographic and radiographic assessments, measurements, and calculations were performed by a single observer who was well trained by a cardiologist and blinded to the dogs' identities.

### *Animals*

Client-owned dogs who were clinically healthy or had MMVD were prospectively included in our study. Dogs were described as clinically healthy based on their medical histories, physical examinations, electrocardiography, radiography, non-invasive blood pressure measurements using the oscillometric method, and transthoracic echocardiography. Dogs were diagnosed as having MMVD based on the presence of mitral valve thickening, or prolapse and mitral regurgitation, as determined by transthoracic echocardiography [34]. Exclusion criteria for this study were the presence of (1) other cardiac diseases; (2) diseases that might increase the pulmonary artery pressure, such as pulmonary disease, thromboembolic disease, and neoplastic disease; (3) diseases that might affect cardiac function, such as endocrine disease and systemic hypertension (systolic blood pressure≥160 mmHg [1]); and/or (4) missing data.

### *Classification*

Dogs with MMVD were divided into three groups based on the American College of Veterinary Internal Medicine (ACVIM) consensus: Stage B1 identified asymptomatic dogs with no or minimal remodeling, Stage B2 identified asymptomatic dogs with significant left heart remodeling based on radiography and echocardiography, and Stage C/D identified symptomatic dogs with current or past clinical signs of heart failure caused by MMVD [21]. Additionally, dogs with MMVD were classified into three PH probability groups according to the ACVIM consensus using echocardiographic findings of the tricuspid valve regurgitation (TR) velocity and anatomical abnormalities of the right heart, pulmonary artery, and caudal vena cava: low, intermediate, and high probability of PH (low, intermediate, and high groups, respectively) [30]. Even in asymptomatic dogs without substantial left heart remodeling due to MMVD, cases with echocardiographic findings indicating increased left atrial pressure were classified into the B1 group and the respective PH probability groups. Increased left atrial pressure was estimated according to increased early-diastolic transmitral flow velocity (>1.4 m/sec) and ratio of early-diastolic transmitral flow velocity to early-diastolic myocardial velocity of the septal mitral annulus (>13) [17, 32, 38]. Peak TR velocity was obtained from the right parasternal long-axis view, short-axis view at the level of the heart base, and/or the left parasternal apical four-chamber view [13, 31, 44]. The average value which was obtained from the highest quality of TR signals in any echocardiographic view was used for the classification. The TR pressure gradient was calculated using the simplified Bernoulli equation. Furthermore, the dogs with TR were classified qualitatively according to severity using color Doppler and continuous wave Doppler methods as previously described: mild TR identified as a small TR jet and a faint parabolic TR jet signal, moderate TR identified as an intermediate TR jet and a dense parabolic TR jet signal, and severe TR identified as a very large central jet or eccentric wall impinging jet and a dense triangular, early peaking TR jet signal [23, 41]. Dogs were diagnosed as having left-sided congestive heart failure, if they showed the radiographic evidence of cardiogenic pulmonary edema characterized by an interstitial and/or alveolar pulmonary pattern in the lung fields [21]. The R-CHF was diagnosed if dogs had radiographic and/or ultrasonographic evidence of ascites, pleural effusion, or pericardial effusion without any other abnormalities than PH that may have been responsible.

### *Clinical examinations*

All dogs underwent a complete physical examination and blood pressure measurement using the oscillometric method on the same day as echocardiographic evaluation. When necessary, they underwent blood, coagulation, and/or neurological examinations to aid in the differential diagnosis of the diseases listed in the exclusion criteria. When dogs had echocardiographic evidence of intracardiac thrombus and smoke-like echo, dogs underwent a coagulation examination. If dogs showed abnormally high values of fibrin/fibrinogen degradation products (>4.0 µg/ml) or D-dimer (>2.0 µg/ml) or both, these dogs were suspected of having thromboembolic disease and were excluded from this study. The differential diagnosis of endocrine disease was performed based on the blood examination (blood chemistry examination and hormone concentration measurement) and abdominal ultrasonography. Especially, dogs with clinical findings associated with hypothyroidism, such as bradycardia, lethargy, weakness, and depression, were measured serum $T_4$ and free $T_4$ concentrations, and those with abnormally low $T_4$ and free $T_4$ values (<1.1 µg/dl and <0.5

ng/dl, respectively) were excluded from this study. If dogs had clinical findings associated with hyperadrenocorticism, such as polydipsia, polyuria, hepatomegaly, and abdominal enlargement, they underwent adrenocorticotropic hormone stimulation test and abdominal ultrasonography, and those with abnormally high cortisol value (post-stimulation: >25 µg/dl) were excluded from this study. Thoracic radiography was performed to evaluate the presence of respiratory abnormalities, CHF, and cardiomegaly. Abdominal ultrasonography was performed to assess the presence of ascites and congestion of the caudal vena cava and hepatic vein using the caudal vena cava subxiphoid point-of-care ultrasound view [25, 42].

### *Echocardiographic evaluation of right heart*

Conventional 2D, M-mode, and Doppler examinations were performed using an echocardiographic system (Vivid E95, GE Healthcare, Tokyo, Japan) and a 3.5–6.9 MHz transducer. Lead II electrocardiography was performed simultaneously and the results were displayed on the images. All data were obtained from at least five consecutive cardiac cycles in the sinus rhythm from non-sedated dogs that were manually restrained in right and left lateral recumbency. All images were analyzed by a single observer who was well trained by a cardiologist using an offline workstation (EchoPAC PC, Version 203, GE Healthcare).

To reduce the effect of respiratory variation, the means of five consecutive cardiac cycles in the sinus rhythm from high-quality images were used for all analyses of the echocardiographic indices of the right heart. The end-diastolic RV internal dimension (RVIDd), end-diastolic and end-systolic RV area (RVEDA and RVESA), right atrial area (RAA), end-diastolic right ventricular wall thickness (RVWTd), and pulmonary artery to aortic diameter ratio (PA/Ao) were measured as the morphological indicators of the right heart. These indices except for PA/Ao were obtained from the left parasternal apical four-chamber view optimized for the right heart (RV focus view) [13, 31, 44]. The RVIDd was measured as the largest diameter at the middle right ventricle parallel to the tricuspid annulus using the B-mode method. The RVEDA and RVESA were measured by tracing the endocardial border of the RV inflow region at end-diastole and end-systole excluding the papillary muscles (Fig. 1A and 1B) [41, 44]. The RAA was also measured by tracing the endocardial border of the right atrium at the end-systole (Fig. 1B) [40]. To eliminate the effect of body sizes, the RVIDd, RVEDA, RVESA, and RAA indices were normalized using the following formulae [13]:

$$\text{RVIDd index}=(\text{RVIDd [mm]})/(\text{body weight [kg]})^{0.327}$$

$$\text{RVEDA index}=(\text{RVEDA [cm}^2\text{]})/(\text{body weight [kg]})^{0.624}$$

$$\text{RVESA index}=(\text{RVESA [cm}^2\text{]})/(\text{body weight [kg]})^{0.628}$$

$$\text{RAA index}=(\text{RAA [cm}^2\text{]})/(\text{body weight [kg]})^{0.714}$$

The RVWTd was measured as the largest diameter of RV free wall at end-diastole using B-mode method (Fig. 1A). The PA/Ao was obtained from the right parasternal short-axis view at the level of pulmonary artery, as previously described (Fig. 1C) [43].

For the assessment of RV function, the following indices were measured: tricuspid annular plane systolic excursion (TAPSE), RV fractional area change (RV FAC), peak velocity of systolic tricuspid annular motion as determined by tissue Doppler (RV S'), and tissue Doppler-derived RV myocardial performance index (RV MPI). These indices were obtained from the RV focus view [13, 31, 44]. The TAPSE was measured using the M-mode image constructed by B-mode cine loops offline as the total displacement of the tricuspid annulus from end-diastole to end-systole (Fig. 1D). The RV FAC was calculated using the RVEDA and RVESA [44]:

$$\text{RV FAC (\%)}=([\text{RVEDA}-\text{RVESA}]/\text{RVEDA}) \times 100.$$

The TAPSE and RV FAC normalized by body weight (TAPSEn and RV FACn, respectively) were calculated using the following formulae [7, 44]:

$$\text{TAPSEn}=(\text{TAPSE})/(\text{body weight [kg]})^{0.33}$$

$$\text{RV FACn}=(\text{RV FAC})/(\text{body weight [kg]})^{-0.097}.$$

The RV S' and RV MPI were obtained from the tissue Doppler imaging-derived lateral tricuspid annular motion wave. The RV S' was measured as the peak systolic velocity of the lateral tricuspid annulus (Fig. 1E) [44]. The RV MPI was measured using the following formula:

$$\text{RV MPI}=(d-c)/c$$

In this formula, c is the duration of the systolic tricuspid annular motion wave, and d is the interval from the end of the late diastolic tricuspid annular motion wave to the onset of the early diastolic tricuspid annular motion wave (Fig. 1E) [31].

### *Two-dimensional speckle tracking echocardiography*

All 2D-STE analyses were performed by the same investigator using the same ultrasound and offline workstation as those for standard echocardiography. The strain and strain rate were obtained from the RV focus view using the left ventricular four-chamber algorithms [48]. The region of interest for 2D-STE was defined by manually tracing the RV endocardial border. Only RV free wall analysis (3seg) was performed by tracing from the level of the lateral tricuspid annulus to the RV apex for the longitudinal strain ($\text{RV-SL}_{3seg}$), as well as strain rate ($\text{RV-SrL}_{3seg}$). Right ventricular global analysis (6seg) was also performed by tracing from the lateral tricuspid annulus to the septal tricuspid annulus (including the interventricular septum) via the RV apex for the 6seg longitudinal strain ($\text{RV-SL}_{6seg}$), and strain rate ($\text{RV-SrL}_{6seg}$) (Fig. 2). Manual adjustments were performed to include and track the entire myocardial thickness over the cardiac cycle when necessary. When the automated software could not track the myocardial regions, the regions of interest were retraced and recalculated. The RV-SL was defined as the absolute value of the negative peak value obtained from the global strain wave calculated automatically. The RV-SrL at systole, early-diastole, and late-diastole (S, E, A, respectively) were obtained from the global strain rate wave calculated automatically. The RV-SrL S was defined as the absolute value of the negative peak value during systole, and the RV-SrL E and A were defined as the peak values obtained from the early- and late-diastolic strain rate waves, respectively [35, 36].

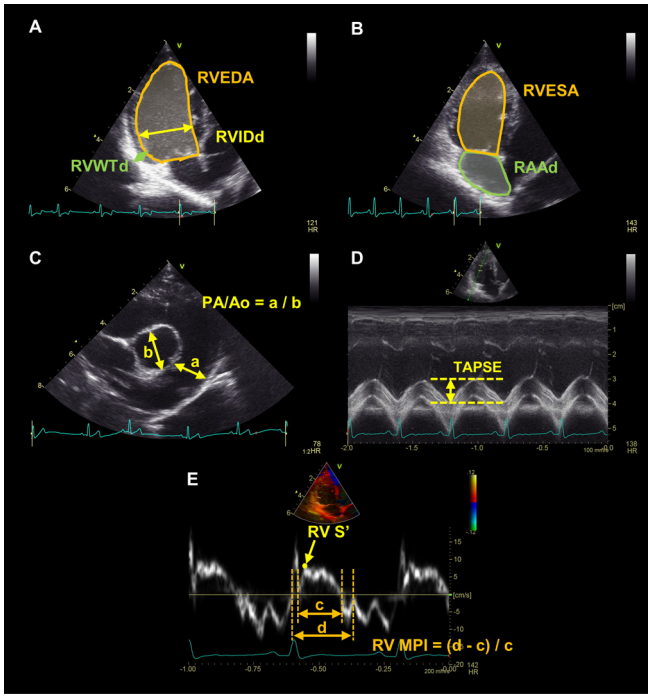


**Fig. 1.** Echocardiographic indices for right heart measured in this study: end-diastolic right ventricular internal dimension (RVIDd), end-diastolic right ventricular area (RVEDA), end-diastolic right ventricular wall thickness (RVWTd) **(A)**, end-systolic right ventricular area (RVESA), right atrial area (RAA) **(B)**, ratio of pulmonary artery dimension to aortic annulus dimension (PA/Ao) **(C)**, tricuspid annular plane systolic excursion (TAPSE) **(D)**, peak velocity of systolic tricuspid annular motion as determined by tissue Doppler (RV S') and right ventricular myocardial performance index **(E)**.

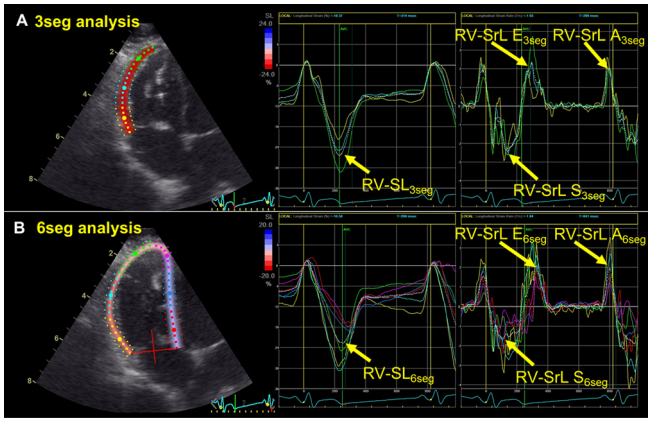


**Fig. 2.** Right ventricular strain (RV-SL) and strain rate (RV-SrL) obtained by two-dimensional speckle tracking echocardiography: RV-SL and RV-SrL of 3-segmental analysis **(A)**, and those of 6-segmental analysis **(B)**.

### *Intra- and inter-observer measurement variability*

Intra-observer measurement variability was performed by the same observer who performed all echocardiographic and radiographic analyses. All echocardiographic indices of the right heart except for the normalized indices from ten dogs, comprising two dogs randomly selected from the normal group and each PH probability group, were measured on different days using the same echocardiogram and heart cycles. A second blinded observer used the same echocardiographic indices to obtain interobserver measurement variability using the same echocardiogram and heart cycles. Two mean values calculated from the same cardiac cycles were used to evaluate the intra- and interobserver measurement variability.

### *Statistical analysis*

All statistical analyses were performed using EZR software version 1.41 [20]. Categorical data were reported as absolute (number) and frequency (percentage). Continuous variables were reported as the mean value ± standard deviation.

The normality of data was tested using a Shapiro-Wilk test. Depending on the expected cell counts of the contingency tables, Fisher's exact test was used to compare categorical variables between the probability of PH group. Continuous variables were compared among the normal group and each probability of PH group using a one way analysis of variance with subsequent pairwise comparisons using the Tukey test for normally distributed data or Kruskal-Wallis test with subsequent pairwise comparisons using the Steel-Dwass test for non-normally distributed data. To identify the relationship between echocardiographic indices and the presence of R-CHF, univariate and multivariate logistic regression analyses were performed. Indices that had $P<0.10$ in the univariate analysis were entered into the multivariate analysis, and those that had coefficients of correlation $|r|>0.7$ were not enrolled owing to multicollinearity. Indices entered into the logistic regression analysis were recorded as odds ratios and their respective 95% confidence intervals (CI). Additionally, receiver operating characteristic curves were created to determine the optimal cutoff values required for the evaluate the association with the presence of R-CHF in the indices that were significant in the multivariate analysis. The cut-off value was defined as that which minimized the distance between the curve and the upper left corner in the receiver operating characteristic curve. Statistical significance for all analyses was set at $P<0.05$.

Intra- and inter-observer measurement variability was quantified by the coefficient of variation (CV) using a root mean square method, as previously described [3]. Low measurement variability was defined as a CV <10.0 [24].

## RESULTS

### *Clinical profiles and standard echocardiography*

A total of 83 dogs—20 healthy dogs and 63 dogs with MMVD—were enrolled in this study comprising the following breeds: Chihuahua (n=21; 25%), mixed breed (n=10; 12%), Toy Poodle (n=6; 7%), Shih Tzu (n=6; 7%), Miniature Dachshund (n=6; 7%), Maltese (n=5; 6%), Papillon (n=4; 5%), Miniature Schnauzer (n=4; 5%), Pomeranian (n=3; 3%), Cavalier King Charles spaniel (n=2; 2%), Chinese Crested dog (n=2; 2%), Norfolk terrier (n=2; 2%), Pekingese (n=2; 2%), Miniature Pinscher (n=2; 2%), and a dog each from eight other breeds. Seventy-four percent of dogs with MMVD were receiving some medical treatment from the referral hospital at the time of examination; angiotensin converting enzyme inhibitors (low: n=12; intermediate: n=13; high: n=20),

pimobendan (low: n=4; intermediate: n=10; high: n=14), pulmonary vasodilators (sildenafil) (low: n=0; intermediate: n=3; high: n=5), loop diuretics (low: n=0; intermediate: n=1; high: n=4), or some combination of those.

All data on the clinical and selected echocardiographic indices, as classified by the probability of PH, are summarized in Table 1. The age, sex, body weight, and heart rate were not significantly different across the normal and the probability of PH groups. The population of severe MMVD (C/D group) and tricuspid valve regurgitation (TR) was significantly higher in the high group (both were $P<0.001$). Nine dogs in the high group (41%) had at least one sign of R-CHF at the time of examination: ascites (n=5), pleural effusion (n=3), pericardial effusion (n=2), or some combination of these. A significantly higher percentage of dogs with R-CHF was treated with angiotensin converting enzyme inhibitors (R-CHF [%]: n=9 [100%]; non-R-CHF [%]; n=41 [52%], $P=0.009$), pimobendan (R-CHF [%]: n=8 [89%]; non-R-CHF [%]; n=22 [28%], $P<0.001$), and sildenafil (R-CHF [%]: n=4 [44%]; non-R-CHF [%]; n=4 [5%], $P=0.003$) compared with that of dogs without R-CHF. There was no significant difference in the percentage of dogs medicated by loop diuretics between the presence or absence of R-CHF (R-CHF [%]: n=2 [29%]; non-R-CHF [%]; n=3 [4%], $P=0.080$).

### *Echocardiographic indices for right heart*

All echocardiographic data of the right heart, as classified by the probability of PH, is summarized in Table 2 and Fig. 3. All morphological indicators of the right heart, including RVIDd index, RVEDA index, RVESA index, and RAA index, were significantly higher only in the high group (Fig. 3A). The TAPSEn was significantly higher in the intermediate and high groups compared with that in the normal group ($P=0.005$ [vs. intermediate group], $P=0.006$ [vs. high group]), and was significantly higher in the intermediate group than that in the low group ($P=0.040$) (Fig. 3B). The RV FACn and RV S' showed no significant differences among the normal and each PH probability group. The RV MPI showed a significant increase in the high group compared with the normal, low, and intermediate groups ($P=0.005$, $P=0.029$, $P=0.033$, respectively) (Fig. 3C).

For the 2D-STE indices, all myocardial segments were included in the statistical analyses (Table 3 and Fig. 3D and 3E). The RV-SrL E of each segment analysis showed significantly lower values in the high group compared with that in the intermediate group (RV-SrL $E_{3seg}$: $P=0.047$; RV-SrL $E_{6seg}$: $P=0.010$). Additionally, RV-SrL $E_{6seg}$ was higher in the intermediate group than that in the normal group ($P=0.041$) (Fig. 3D). The RV-SrL A of each segment analysis showed no significant difference among each PH probability group. The RV-SL of each segment analysis was significantly lower in the high group than that in the low and intermediate groups (RV-$SL_{3seg}$: $P=0.049$, $P=0.008$, respectively; RV-$SL_{6seg}$: $P=0.027$, $P=0.001$, respectively) (Fig. 3E). The RV-SrL $S_{3seg}$ was significantly higher in the intermediate group than that in the normal and high groups ($P=0.048$, $P=0.020$, respectively) Whereas, RV-SrL $S_{6seg}$ was significantly lower in the high group than that in the low and intermediate groups ($P=0.021$, $P=0.005$, respectively).

Table 4 shows the results comparing echocardiographic indices according to the presence or absence of R-CHF. All RV morphological indices, including RVIDd index, RVEDA index, RVESA index, RAA index, RVWTd, and PA/Ao, were significantly higher in dogs with R-CHF. The RV FACn, RV-SrL S, RV-SrL $E_{6seg}$, and RV-$SL_{6seg}$ were significantly lower in dogs with R-CHF. The RV MPI was significantly higher in dogs with R-CHF. There was no significant difference in TAPSEn, RV S', RV-SrL $E_{3seg}$, RV-SrL A, RV-SrL E/A, and RV-$SL_{3seg}$ between dogs with and without R-CHF.

### *Intra- and inter-observer measurement variability*

The measurement variability-related results are summarized in Table 5. In terms of the intra-observer measurement variability, all of the indices except for RV-SrL $E_{3seg}$ had low measurement variabilities [24]. However, RVEDA, RVESA, TAPSE, RV FAC, RV-SrL $E_{3seg}$, RV-SrL $A_{3seg}$, and RV-SrL $A_{6seg}$ did not meet the definition of low measurement variability for inter-observer measurement variability [24].

### *Logistic regression analyses*

For the results of the univariate models that evaluated the association between echocardiographic indices and the presence of R-CHF, an association was observed between the presence of R-CHF and increased RVIDd index, RVEDA index, RVESA, RAA

**Table 1.** Clinical and selected echocardiographic variables obtained from normal dogs and dogs with myxomatous mitral valve disease

| Variable | Group | | | | *P** |
|---|---|---|---|---|---|
| | Normal | Low | Intermediate | High | |
| n | 20 | 25 | 16 | 22 | |
| Age (year) | 11.2 ± 2.2 | 11.6 ± 2.7 | 11.4 ± 2.4 | 13.0 ± 1.8 | 0.052 |
| Sex (Male, Female) | 8, 12 | 14, 10 | 9, 7 | 11, 12 | 0.616 |
| Body weight (kg) | 6.2 ± 4.0 | 5.6 ± 3.5 | 4.8 ± 1.9 | 5.7 ± 4.6 | 0.769 |
| Heart rate (bpm) | 124 ± 30 | 118 ± 32 | 122 ± 30 | 137 ± 35 | 0.350 |
| ACVIM (B1, B2, C/D) | | 12, 9, 4 | 4, 9, 3 | 0, 7, 15 | <0.001 |
| TR severity (mild, moderate, severe) | 0, 0, 0 | 15, 2, 0 | 1, 13, 2 | 6, 6, 10 | <0.001 |
| R-CHF (present, absent) | 0, 20 | 0, 25 | 0, 16 | 9, 13 | <0.001 |

High: high probability of PH; Intermediate: intermediate probability of PH; Low: low probability of PH; PH: pulmonary hypertension; R-CHF: right-sided congestive heart failure; TR: tricuspid valve regurgitation. Continuous variables are displayed as mean ± standard deviation. *: *P* value of one way analysis of variance or Kruskal-Wallis test for continuous variables and Fisher's exact tests for categorical variables.

**Table 2.** Echocardiographic variables for the right heart in normal dogs and dogs with myxomatous mitral valve disease

| Variable | Group | | | | *P* |
|---|---|---|---|---|---|
| | Normal | Low | Intermediate | High | |
| RVEDA index | 0.80 ± 0.21 | 0.76 ± 0.19 | 0.83 ± 0.14 | 1.18 ± 0.37[a,b,c] | <0.001 |
| RVESA index | 0.41 ± 0.15 | 0.39 ± 0.10 | 0.41 ± 0.10 | 0.62 ± 0.23[a,b,c] | <0.001 |
| RAA index | 0.46 ± 0.1 | 0.45 ± 0.15 | 0.56 ± 0.18 | 0.94 ± 0.49[a,b,c] | <0.001 |
| RVWTd (mm) | 3.6 ± 0.4 | 3.5 ± 0.7 | 3.7 ± 0.8 | 4.4 ± 0.9[a,b,c] | <0.001 |
| PA/Ao | 0.81 ± 0.2 | 0.8 ± 0.1 | 0.91 ± 0.1[b] | 1.00 ± 0.2[a,b] | 0.004 |
| RV FACn | 58.7 ± 11.1 | 55.5 ± 10.2 | 58.2 ± 7.6 | 54.6 ± 11.5 | 0.605 |
| RV S' (cm/sec) | 10.4 ± 2.7 | 10.7 ± 2.8 | 11.8 ± 2.0 | 12.5 ± 4.6 | 0.165 |
| RV MPI | 0.44 ± 0.2 | 0.45 ± 0.2 | 0.43 ± 0.1 | 0.61 ± 0.2[a,b,c] | 0.002 |

High: high probability of PH; Intermediate: intermediate probability of PH; Low: low probability of PH; PA/Ao: pulmonary artery to aortic diameter ratio; RAA index: right atrial area normalized by body weight; RV: right ventricular; RV FACn: RV fractional area change normalized by body weight; RV S': peak systolic velocity of lateral tricuspid annular motion; RVEDA index: end-diastolic RV area normalized by body weight; RVESA index: end-systolic RV area normalized by body weight; RVWTd: end-diastolic RV wall thickness. Continuous variables are displayed as mean ± standard deviation. a; the value is significantly different from the normal, b; the value is significantly different from the low probability of PH group, c; the value is significantly different from the intermediate probability of PH group.

**Table 3.** Two-dimensional speckle tracking echocardiography-derived indices in normal dogs and dogs with myxomatous mitral valve disease

| Variable | Group | | | | *P* |
|---|---|---|---|---|---|
| | Normal | Low | Intermediate | High | |
| RV-SrL $S_{3seg}$ (1/sec) | 4.2 ± 1.5 | 5.1 ± 2.1 | 5.9 ± 2.3 | 3.7 ± 1.4[b,c] | 0.002 |
| RV-SrL $E_{3seg}$ (1/sec) | 2.6 ± 1.3 | 3.6 ± 2.3 | 4.0 ± 2.1 | 3.0 ± 1.7[c] | 0.038 |
| RV-SrL $A_{3seg}$ (1/sec) | 3.5 ± 1.5 | 4.1 ± 2.4 | 3.9 ± 1.0 | 3.7 ± 1.7 | 0.622 |
| RV-SrL $E/A_{3seg}$ | 0.8 ± 0.3 | 1.1 ± 0.5 | 1.1 ± 0.8 | 1.1 ± 0.5 | 0.269 |
| RV-$SL_{3seg}$ (%) | 26.9 ± 7.8 | 29.4 ± 7.8 | 30.7 ± 7.3 | 24.8 ± 6.7[b,c] | 0.011 |
| RV-SrL $S_{6seg}$ (1/sec) | 3.2 ± 1.0 | 3.6 ± 1.1 | 4.1 ± 1.4 | 2.8 ± 1.0[b,c] | 0.004 |
| RV-SrL $E_{6seg}$ (1/sec) | 2.3 ± 1.0 | 2.7 ± 1.3 | 3.4 ± 1.2[a] | 2.2 ± 1.0[c] | 0.012 |
| RV-SrL $A_{6seg}$ (1/sec) | 2.5 ± 1.0 | 3.1 ± 1.5 | 3.3 ± 0.8 | 2.6 ± 1.2 | 0.072 |
| RV-SrL $E/A_{6seg}$ | 1.0 ± 0.5 | 1.2 ± 0.6 | 1.1 ± 0.6 | 1.2 ± 0.5 | 0.472 |
| RV-$SL_{6seg}$ (%) | 23.2 ± 6.1 | 25.3 ± 5.7 | 27.8 ± 5.3 | 20.2 ± 6.1[b,c] | 0.004 |

3seg: right ventricular free wall analysis; 6seg: right ventricular global analysis; High: high probability of PH; Intermediate: intermediate probability of PH; Low: low probability of PH; PH: pulmonary hypertension; RV: right ventricular; RV-SL: RV longitudinal strain; RV-SrL A: late-diastolic RV strain rate; RV-SrL E: early-diastolic RV strain rate; RV-SrL S: systolic RV strain rate. Continuous variables are displayed as mean ± standard deviation. a; the value is significantly different from the normal, b; the value is significantly different from the low probability of PH group, c; the value is significantly different from the intermediate probability of PH group.

index, RVWTd, PA/Ao, and RV MPI, and decreased RV FACn, RV-SrL $S_{3seg}$, RV-$SL_{6seg}$, RV-SrL $S_{6seg}$, and RV-SrL $E_{6seg}$ (Table 6). After adjusting for confounding factors, four indices, including RVIDd index, RVWTd, RV MPI, and RV-$SL_{6seg}$, were included in the multivariate model, and RVIDd index and RV MPI remained significant in the multivariate model. The optimal cutoff of RVIDd index and RV MPI were 8.487 (area under the curve [95% confidence interval], 0.98 [0.96−1.00]; sensitivity, 0.89; specificity, 0.99) and 0.4593 (area under the curve [95% confidence interval], 0.73 [0.57−0.92]; sensitivity, 0.78; specificity, 0.67), respectively (Fig. 4).

## DISCUSSION

Our results of 2D-STE indices demonstrated that RV function, not only systolic function but also diastolic function, was increased in the intermediate probability of PH group than the normal group. Whereas, RV systolic and diastolic function were significantly impaired in dogs with high probability of PH, which might reflect the substantial increase of pulmonary artery pressure and RV myocardial dysfunction. Additionally, dogs with R-CHF showed significantly increased RV MPI, which could detect both systolic and diastolic disorders in the right ventricle. These non-invasive variables for RV function might provide additional information to monitor the PH progression and detect the presence of R-CHF.

In this study, conventional echocardiographic indices for RV systolic function, such as TAPSEn and RV S', were higher in the intermediate group compared with the normal group. However, there was no significant decline in these conventional echocardiographic indices for RV function in the high group, although the 2D-STE indices showed significant worsening. The conventional echocardiographic indices, such as TAPSEn, RV FACn, RV S', were easily affected by heart rate, volume overload, and/or ventricular interdependence in addition to intrinsic RV function [16, 18]. These influences might prevent the detection of RV systolic dysfunction in the high group using conventional echocardiographic indices, including TAPSEn, RV FACn, and RV S'. Whereas 2D-STE-derived RV-SrL S and RV-SL were significantly lower in the high group compared with the low and intermediate groups. The 2D-STE could evaluate the precise myocardial function with low effects from the heart rate, volume overload, and

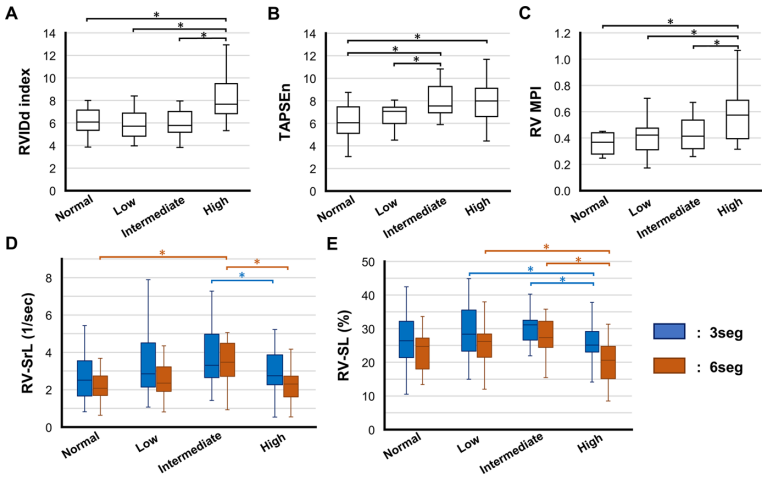


**Fig. 3.** Box and Whisker plots of selected echocardiographic indices with statistically significant differences among various pulmonary hypertension probability groups: end-diastolic right ventricular internal dimension normalized by body weight (RVIDd index) **(A)**, tricuspid annular plane systolic excursion normalized by body weight (TAPSEn) **(B)**, right ventricular myocardial performance index **(C)**, early-diastolic right ventricular strain rate (RV-SrL E) **(D)**, and right ventricular strain (RV-SL) **(E)**. The Whiskers indicate the range of values obtained, the box extends from the 25th to the 75th percentile, and the horizontal bar in the box represents the median. For the RV-SrL E and RV-SL, blue box plots represent 3seg, and orange box plots represent 6seg. *; Values differed significantly between pulmonary hypertension probability groups. The sign in blue and orange indicate significant differences in 3seg and 6seg, respectively.

**Table 4.** Echocardiographic variables for the right heart in dogs with and without right-sided congestive heart failure

| Variables | Group | | *P* |
|---|---|---|---|
| | R-CHF (+) | R-CHF (-) | |
| RVIDd index | 10.2 ± 2.3 | 6.2 ± 1.3 | <0.001 |
| RVEDA index | 1.40 ± 0.4 | 0.83 ± 0.2 | 0.001 |
| RVESA index | 0.77 ± 0.2 | 0.42 ± 0.1 | <0.001 |
| RAA index | 1.24 ± 0.6 | 0.52 ± 0.2 | <0.001 |
| RVWTd (mm) | 4.8 ± 0.9 | 3.6 ± 0.7 | <0.001 |
| PA/Ao | 1.1 ± 0.2 | 0.86 ± 0.2 | 0.002 |
| TAPSEn | 7.2 ± 1.5 | 7.2 ± 1.8 | 0.823 |
| RV FACn | 49.8 ± 13.3 | 57.5 ± 9.7 | 0.027 |
| RV S' (cm/sec) | 12.9 ± 4.7 | 11.1 ± 3.1 | 0.378 |
| RV MPI | 0.67 ± 0.2 | 0.46 ± 0.2 | 0.009 |
| RV-SrL $S_{3seg}$ (1/sec) | 3.4 ± 1.3 | 4.7 ± 2.1 | 0.027 |
| RV-SrL $E_{3seg}$ (1/sec) | 2.9 ± 1.1 | 3.4 ± 2.1 | 0.319 |
| RV-SrL $A_{3seg}$ (1/sec) | 3.9 ± 1.8 | 3.8 ± 1.8 | 0.694 |
| RV-SrL $E/A_{3seg}$ | 1.0 ± 0.4 | 1.0 ± 0.8 | 0.818 |
| RV-$SL_{3seg}$ (%) | 25.9 ± 5.6 | 28.1 ± 7.9 | 0.444 |
| RV-SrL $S_{6seg}$ (1/sec) | 2.4 ± 0.9 | 3.5 ± 1.2 | 0.010 |
| RV-SrL $E_{6seg}$ (1/sec) | 1.9 ± 0.8 | 2.7 ± 1.2 | 0.044 |
| RV-SrL $A_{6seg}$ (1/sec) | 2.8 ± 1.3 | 2.9 ± 1.2 | 0.694 |
| RV-SrL $E/A_{6seg}$ | 1.0 ± 0.5 | 1.1 ± 0.8 | 0.860 |
| RV-$SL_{6seg}$ (%) | 18.8 ± 5.9 | 24.7 ± 6.2 | 0.007 |

3seg: right ventricular free wall analysis; 6seg: right ventricular global analysis; PA/Ao: pulmonary artery to aortic diameter ratio; RAA: right atrial area; R-CHF: right-sided congestive heart failure; RV FAC: right ventricular fractional area change; RV MPI: right ventricular myocardial performance index; RV S': peak systolic velocity of lateral tricuspid annular motion; RVEDA: end-diastolic right ventricular area; RVESA: end-systolic right ventricular area; RVIDd: end-diastolic right ventricular internal dimension; RV-SL: right ventricular strain; RV-SrL A: late-diastolic right ventricular strain rate; RV-SrL E: early-diastolic right ventricular strain rate; RV-SrL S: systolic right ventricular strain rate; RVWTd: end-diastolic right ventricular wall thickness; TAPSE: tricuspid annular plane systolic excursion. Continuous variables are displayed as mean ± standard deviation.

**Table 5.** Intra- and inter-observer measurement variability for echocardiographic variables

| Variables | Intra-observer | Inter-observer |
|---|---|---|
| | CV (%) | CV (%) |
| RVIDd (mm) | 5.1 | 9.0 |
| RVEDA ($cm^2$) | 4.8 | 13.9 |
| RVESA ($cm^2$) | 7.2 | 26.0 |
| RAA ($cm^2$) | 6.9 | 8.9 |
| RVWTd (mm) | 5.4 | 7.8 |
| PA/Ao | 7.2 | 8.9 |
| TAPSE (mm) | 8.3 | 9.3 |
| RV FAC (%) | 7.2 | 13.8 |
| RV S' (cm/sec) | 4.0 | 4.3 |
| RV MPI | 8.5 | 9.2 |
| RV-SrL $S_{3seg}$ (1/sec) | 7.2 | 11.3 |
| RV-SrL $E_{3seg}$ (1/sec) | 10.3 | 9.2 |
| RV-SrL $A_{3seg}$ (1/sec) | 5.5 | 13.0 |
| RV-$SL_{3seg}$ (%) | 4.8 | 5.7 |
| RV-SrL $S_{6seg}$ (1/sec) | 6.9 | 9.2 |
| RV-SrL $E_{6seg}$ (1/sec) | 9.1 | 9.8 |
| RV-SrL $A_{6seg}$ (1/sec) | 7.7 | 12.5 |
| RV-$SL_{6seg}$ (%) | 6.9 | 6.9 |

3seg: right ventricular free wall analysis; 6seg: right ventricular global analysis; CV: coefficient of variation; PA/Ao: pulmonary artery to aortic diameter ratio; RAA: right atrial area; RV FAC: right ventricular fractional area change; RV MPI: right ventricular myocardial performance index; RV S': peak systolic velocity of lateral tricuspid annular motion; RVEDA: end-diastolic right ventricular area; RVESA: end-systolic right ventricular area; RVIDd: end-diastolic right ventricular internal dimension; RV-SL: right ventricular strain; RV-SrL A: late-diastolic right ventricular strain rate; RV-SrL E: early-diastolic right ventricular strain rate; RV-SrL S: systolic right ventricular strain rate; RVWTd: end-diastolic right ventricular wall thickness; TAPSE: tricuspid annular plane systolic excursion.

ventricular interdependence [2, 35]. Our results suggested that 2D-STE-derived RV-SL might reflect the precise RV systolic dysfunction which could not be detected by conventional echocardiographic indices.

This is the first study to evaluate the diastolic function of the RV using RV-SrL E of 2D-STE in dogs with MMVD. The RV-SrL $E_{6seg}$ showed a significant increase in the intermediate group compared with that in the normal group, and a significant decrease in the high group compared with that in the intermediate group, which indicated a similar tendency to RV systolic function assessed by RV-SrL S and RV-SL. Our results suggested that RV diastolic function might also be increased compensatory in the intermediate

**Table 6.** Results of logistic regression analysis to evaluate the association between echocardiographic indices and the presence of right-sided congestive heart failure

| Variables | Univariate analysis | | Multivariate analysis | |
|---|---|---|---|---|
| | non-adjusted odds ratio (95% CI) | *P* | adjusted odds ratio (95% CI) | *P* |
| RVIDd index | 9.25 (1.92–44.61) | <0.001 | 12.5 (1.85–84.7) | 0.01 |
| RVEDA index (0.1) | 3.71 (1.43–9.62) | <0.001 | | |
| RVESA index (0.1) | 8.40 (2.10–33.70) | <0.001 | | |
| RAA index (0.1) | 2.26 (1.36–3.77) | <0.001 | | |
| RVWTd (0.1 mm) | 4.53 (1.85–11.10) | <0.001 | | |
| PA/Ao (0.1) | 2.07 (1.34–3.20) | <0.001 | | |
| RV FACn | 1.08 (1.00–1.16) | 0.032 | | |
| RV MPI (0.1) | 1.44 (1.09–1.91) | 0.009 | 1.76 (1.02–3.39) | 0.049 |
| RV-SrL $S_{3seg}$ (0.1/sec) | 1.05 (1.00–1.11) | 0.036 | | |
| RV-$SL_{6seg}$ (%) | 1.15 (1.03–1.30) | 0.012 | | |
| RV-SrL $S_{6seg}$ (0.1/sec) | 1.10 (1.01–1.20) | 0.009 | | |
| RV-SrL $E_{6seg}$ (0.1/sec) | 1.06 (1.01–1.14) | 0.041 | | |

6seg: right ventricular global analysis; CI: confidence interval; PA/Ao: pulmonary artery to aortic diameter ratio; RAA index: right atrial area normalized by body weight; RV: right ventricular; RV FACn: RV fractional area change normalized by body weight; RV MPI: RV myocardial performance index; RVEDA index: end-diastolic RV area normalized by body weight; RVESA index: end-systolic RV area normalized by body weight; RVIDd index: end-diastolic RV internal dimension normalized by body weight; RV-SrL E: early-diastolic RV strain rate; RV-SL: RV strain.

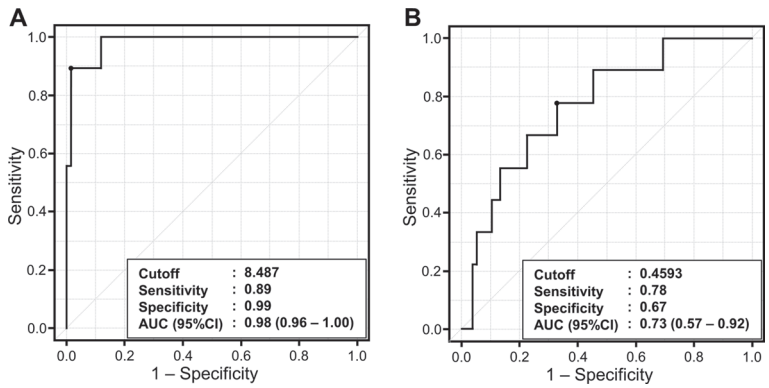


**Fig. 4.** Receiver operating characteristic curves of end-diastolic right ventricular internal dimension normalized by body weight **(A)** and right ventricular myocardial performance index **(B)** to predict the presence of right-sided congestive heart failure.

group, but impaired to the same degree as the normal group in the high group. However, unlike the previous human study, RV diastolic dysfunction preceding systolic dysfunction was not observed in this study [27]. The difference in the degree of RV remodeling and RV compensation might affect the results. In this study, only dogs in the high group had substantial RV remodeling, including hypertrophy and dilatation, which might result in increased RV stiffness and hence RV diastolic dysfunction [10]. Consequently, our findings suggest that temporarily activated RV diastolic function may also be worsened in association with PH progression as well as RV systolic dysfunction. Further studies that evaluate the RV diastolic function using a right heart catheterization in dogs with PH are expected in the future.

Regarding the results of 2D-STE indices, the 6seg analyses showed more drastic changes in cases with high probability of PH, although the 3seg analyses had the same tendency. There has still been controversy surrounding whether 2D-STE analysis for RV function should include interventricular septum [6, 26]. Several experimental studies have reported that the interventricular septum plays an important role in the cardiac output of the right ventricle [9, 33]. Naturally, the chronic pressure overload due to PH would induce entire RV remodeling, and the low cardiac output from the left ventricle associated with MMVD could also damage the myocardium extensively [11]. Therefore, our results suggest that the 6seg analysis might be more useful to assess RV function in dogs with MMVD. However, myocardial function in the interventricular septum might reflect the left ventricular function. Further studies that include the assessment of left ventricular function are warranted in the future.

In this study, the various echocardiographic indices were significantly worsened in dogs with R-CHF. In particular, increased RV MPI was significantly relevant to the presence of R-CHF. The RV MPI reflects the global RV myocardial function, including systolic and diastolic function, and that measured by pulsed-wave Doppler is considered to provide prognostic information in dogs with MMVD [28, 37]. In this study, dogs in the high group showed a significant worsening in RV-SrL S, E, and RV-SL. Our study indicated that the tissue Doppler-derived RV MPI, which could detect both RV systolic and diastolic dysfunction, might also be a clinically useful tool to predict the presence of R-CHF as well as that measured by pulsed-wave Doppler. In addition to RV MPI, RVIDd index showed a significant association in the multivariate analysis. As a previous human study described, RV dilatation would be induced to maintain stroke volume in dogs with RV systolic dysfunction [8]. Therefore, RV dysfunction and associated RV dilatation might provide important information about the presence of R-CHF in dogs with post-capillary PH.

This study had some limitations. First, since the right heart catheterization is the gold standard to evaluate RV function, it was unclear whether 2D-STE derived RV-SL and RV-SrL could detect the intrinsic RV function. Second, few cases of misdiagnosis may have occurred in some dogs with R-CHF. Since all dogs did not undergo complete abdominal ultrasonography, we may not have identified some dogs with mild ascites. Third, the effects of medication could not be considered in dogs with MMVD. Some drugs, such as cardiotonic (pimobendan), pulmonary vasodilators (sildenafil), and diuretics, might affect RV function indices by changing the pressure and volume loads against the right heart. Fourth, the dogs were diagnosed with PH based on the TR pressure gradient and echocardiographic findings of right heart remodeling, although catheterization is the gold standard for PH diagnosis.

Substantially impaired RV function may lead to the underestimation of the peak TR velocity and PH probability. Additionally, because not all dogs have undergone complete differential diagnosis including pathological examination, we might not be able to completely rule out the diseases that could elevate PAP other than MMVD [30]. Furthermore, because coagulation examination was not performed in all dogs, pulmonary thromboembolism might potentially contribute to the increase of PAP. Finally, our study enrolled a relatively small study population of dogs with R-CHF. Unfortunately, there were only a few dogs with post-capillary PH that might progress to pulmonary vascular remodeling secondary to MMVD. Although small sample size might affect the results especially in the multivariate model, our study however could assess and compare precise right heart morphology and function of dogs with post-capillary PH.

In conclusion, 2D-STE indices could detect the change in precise RV function (both systolic and diastolic function) with the progression of PH. Additionally, increased RV MPI, which would reflect RV systolic and diastolic dysfunction, and RV dilatation would be associated with the presence of R-CHF in dogs with post-capillary PH. Additional studies that include more dogs with severe post-capillary PH are expected to further validate our findings.

CONFLICT OF INTEREST. There are no conflicts of interest to declare.

ACKNOWLEDGMENTS. The authors would like to express their deepest appreciation to Haruka Kanno, Hatsumi Endo, and Kana Yanagisawa for their technical assistance. This work was partially supported by the Japanese Society for the Promotion of Science KAKENHI [Grant Number 20K15667].

## REFERENCES

1. Acierno, M. J., Brown, S., Coleman, A. E., Jepson, R. E., Papich, M., Stepien, R. L. and Syme, H. M. 2018. ACVIM consensus statement: Guidelines for the identification, evaluation, and management of systemic hypertension in dogs and cats. *J. Vet. Intern. Med.* **32**: 1803–1822. [Medline] [CrossRef]
2. Amundsen, B. H., Helle-Valle, T., Edvardsen, T., Torp, H., Crosby, J., Lyseggen, E., Støylen, A., Ihlen, H., Lima, J. A. C., Smiseth, O. A. and Slørdahl, S. A. 2006. Noninvasive myocardial strain measurement by speckle tracking echocardiography: validation against sonomicrometry and tagged magnetic resonance imaging. *J. Am. Coll. Cardiol.* **47**: 789–793. [Medline] [CrossRef]
3. Bland, J. M. and Altman, D. G. 1996. Measurement error proportional to the mean. *BMJ* **313**: 106–106. [Medline] [CrossRef]
4. Borgarelli, M., Abbott, J., Braz-Ruivo, L., Chiavegato, D., Crosara, S., Lamb, K., Ljungvall, I., Poggi, M., Santilli, R. A. and Haggstrom, J. 2015. Prevalence and prognostic importance of pulmonary hypertension in dogs with myxomatous mitral valve disease. *J. Vet. Intern. Med.* **29**: 569–574. [Medline] [CrossRef]
5. Chapel, E. H., Scansen, B. A., Schober, K. E. and Bonagura, J. D. 2018. Echocardiographic estimates of right ventricular systolic function in dogs with myxomatous mitral valve disease. *J. Vet. Intern. Med.* **32**: 64–71. [Medline] [CrossRef]
6. Chetboul, V., Damoiseaux, C., Lefebvre, H. P., Concordet, D., Desquilbet, L., Gouni, V., Poissonnier, C., Pouchelon, J. L. and Tissier, R. 2018. Quantitative assessment of systolic and diastolic right ventricular function by echocardiography and speckle-tracking imaging: a prospective study in 104 dogs. *J. Vet. Sci.* **19**: 683–692. [Medline] [CrossRef]
7. Cornell, C. C., Kittleson, M. D., Della Torre, P., Häggström, J., Lombard, C. W., Pedersen, H. D., Vollmar, A. and Wey, A. 2004. Allometric scaling of M-mode cardiac measurements in normal adult dogs. *J. Vet. Intern. Med.* **18**: 311–321. [Medline] [CrossRef]
8. Dandel, M. and Hetzer, R. 2016. Echocardiographic assessment of the right ventricle: Impact of the distinctly load dependency of its size, geometry and performance. *Int. J. Cardiol.* **221**: 1132–1142. [Medline] [CrossRef]
9. Donald, D. E. and Essex, H. E. 1954. Pressure studies after inactivation of the major portion of the canine right ventricle. *Am. J. Physiol.* **176**: 155–161. [Medline] [CrossRef]
10. Douglas, P. S. and Tallant, B. 1991. Hypertrophy, fibrosis and diastolic dysfunction in early canine experimental hypertension. *J. Am. Coll. Cardiol.* **17**: 530–536. [Medline] [CrossRef]
11. Falk, T., Ljungvall, I., Zois, N. E., Höglund, K., Olsen, L. H., Pedersen, H. D. and Häggström, J. 2013. Cardiac troponin-I concentration, myocardial arteriosclerosis, and fibrosis in dogs with congestive heart failure because of myxomatous mitral valve disease. *J. Vet. Intern. Med.* **27**: 500–506. [Medline] [CrossRef]
12. Gaynor, S. L., Maniar, H. S., Bloch, J. B., Steendijk, P. and Moon, M. R. 2005. Right atrial and ventricular adaptation to chronic right ventricular pressure overload. *Circulation* **112** Suppl: I212–I218. [Medline] [CrossRef]
13. Gentile-Solomon, J. M. and Abbott, J. A. 2016. Conventional echocardiographic assessment of the canine right heart: reference intervals and repeatability. *J. Vet. Cardiol.* **18**: 234–247. [Medline] [CrossRef]
14. Guazzi, M. and Naeije, R. 2017. Pulmonary hypertension in heart failure: pathophysiology, pathobiology, and emerging clinical perspectives. *J. Am. Coll. Cardiol.* **69**: 1718–1734. [Medline] [CrossRef]
15. Hoeper, M. M., Bogaard, H. J., Condliffe, R., Frantz, R., Khanna, D., Kurzyna, M., Langleben, D., Manes, A., Satoh, T., Torres, F., Wilkins, M. R. and Badesch, D. B. 2013. Definitions and diagnosis of pulmonary hypertension. *J. Am. Coll. Cardiol.* **62** Suppl: D42–D50. [Medline] [CrossRef]
16. Hsiao, S. H., Lin, S. K., Wang, W. C., Yang, S. H., Gin, P. L. and Liu, C. P. 2006. Severe tricuspid regurgitation shows significant impact in the relationship among peak systolic tricuspid annular velocity, tricuspid annular plane systolic excursion, and right ventricular ejection fraction. *J. Am. Soc. Echocardiogr.* **19**: 902–910. [Medline] [CrossRef]
17. Ishikawa, T., Fukushima, R., Suzuki, S., Miyaishi, Y., Nishimura, T., Hira, S., Hamabe, L. and Tanaka, R. 2011. Echocardiographic estimation of left atrial pressure in beagle dogs with experimentally-induced mitral valve regurgitation. *J. Vet. Med. Sci.* **73**: 1015–1024. [Medline] [CrossRef]
18. Johnson, L., Boon, J. and Orton, E. C. 1999. Clinical characteristics of 53 dogs with Doppler-derived evidence of pulmonary hypertension: 1992-1996. *J. Vet. Intern. Med.* **13**: 440–447. [Medline]
19. Kaga, S., Mikami, T., Onozuka, H., Omotehara, S., Abe, A., Yamada, S., Okada, M., Komatsu, H., Inoue, M., Yokoyama, S., Nishida, M., Shimizu, C., Matsuno, K. and Tsutsui, H. 2009. Right ventricular diastolic dysfunction in patients with left ventricular hypertrophy: analysis of right ventricular myocardial relaxation using two-dimensional speckle tracking imaging. *J. Echocardiogr.* **7**: 25–33. [Medline] [CrossRef]
20. Kanda, Y. 2013. Investigation of the freely available easy-to-use software 'EZR' for medical statistics. *Bone Marrow Transplant.* **48**: 452–458. [Medline] [CrossRef]

21. Keene, B. W., Atkins, C. E., Bonagura, J. D., Fox, P. R., Häggström, J., Fuentes, V. L., Oyama, M. A., Rush, J. E., Stepien, R. and Uechi, M. 2019. ACVIM consensus guidelines for the diagnosis and treatment of myxomatous mitral valve disease in dogs. *J. Vet. Intern. Med.* **33**: 1127–1140. [Medline] [CrossRef]
22. Kellihan, H. B. and Stepien, R. L. 2012. Pulmonary hypertension in canine degenerative mitral valve disease. *J. Vet. Cardiol.* **14**: 149–164. [Medline] [CrossRef]
23. Lancellotti, P., Moura, L., Pierard, L. A., Agricola, E., Popescu, B. A., Tribouilloy, C., Hagendorff, A., Monin, J. L., Badano, L., Zamorano, J. L., European Association of Echocardiography. 2010. European Association of Echocardiography recommendations for the assessment of valvular regurgitation. Part 2: mitral and tricuspid regurgitation (native valve disease). *Eur. J. Echocardiogr.* **11**: 307–332. [Medline] [CrossRef]
24. Landis, J. R. and Koch, G. G. 1977. The measurement of observer agreement for categorical data. *Biometrics* **33**: 159–174. [Medline] [CrossRef]
25. Lisciandro, G. R. 2016. The use of the diaphragmatico-hepatic (DH) views of the abdominal and thoracic focused assessment with sonography for triage (AFAST/TFAST) examinations for the detection of pericardial effusion in 24 dogs (2011–2012). *J. Vet. Emerg. Crit. Care (San Antonio)* **26**: 125–131. [Medline] [CrossRef]
26. Morita, T., Nakamura, K., Osuga, T., Yokoyama, N., Morishita, K., Sasaki, N., Ohta, H. and Takiguchi, M. 2017. Changes in right ventricular function assessed by echocardiography in dog models of mild RV pressure overload. *Echocardiography* **34**: 1040–1049. [Medline] [CrossRef]
27. Murch, S. D., La Gerche, A., Roberts, T. J., Prior, D. L., MacIsaac, A. I. and Burns, A. T. 2015. Abnormal right ventricular relaxation in pulmonary hypertension. *Pulm. Circ.* **5**: 370–375. [Medline] [CrossRef]
28. Nakamura, K., Morita, T., Osuga, T., Morishita, K., Sasaki, N., Ohta, H. and Takiguchi, M. 2016. Prognostic value of right ventricular tei index in dogs with myxomatous mitral valvular heart disease. *J. Vet. Intern. Med.* **30**: 69–75. [Medline] [CrossRef]
29. Rain, S., Handoko, M. L., Trip, P., Gan, C. T. J., Westerhof, N., Stienen, G. J., Paulus, W. J., Ottenheijm, C. A. C., Marcus, J. T., Dorfmüller, P., Guignabert, C., Humbert, M., Macdonald, P., Dos Remedios, C., Postmus, P. E., Saripalli, C., Hidalgo, C. G., Granzier, H. L., Vonk-Noordegraaf, A., van der Velden, J. and de Man, F. S. 2013. Right ventricular diastolic impairment in patients with pulmonary arterial hypertension. *Circulation* **128**: 2016–2025, 1–10. [Medline] [CrossRef]
30. Reinero, C., Visser, L. C., Kellihan, H. B., Masseau, I., Rozanski, E., Clercx, C., Williams, K., Abbott, J., Borgarelli, M. and Scansen, B. A. 2020. ACVIM consensus statement guidelines for the diagnosis, classification, treatment, and monitoring of pulmonary hypertension in dogs. *J. Vet. Intern. Med.* **34**: 549–573. [Medline] [CrossRef]
31. Rudski, L. G., Lai, W. W., Afilalo, J., Hua, L., Handschumacher, M. D., Chandrasekaran, K., Solomon, S. D., Louie, E. K. and Schiller, N. B. 2010. Guidelines for the echocardiographic assessment of the right heart in adults: a report from the American Society of Echocardiography endorsed by the European Association of Echocardiography, a registered branch of the European Society of Cardiology, and the Canadian Society of Echocardiography. *J. Am. Soc. Echocardiogr.* **23**: 685–713, quiz 786–788. [Medline] [CrossRef]
32. Sargent, J., Muzzi, R., Mukherjee, R., Somarathne, S., Schranz, K., Stephenson, H., Connolly, D., Brodbelt, D. and Fuentes, V. L. 2015. Echocardiographic predictors of survival in dogs with myxomatous mitral valve disease. *J. Vet. Cardiol.* **17**: 1–12. [Medline] [CrossRef]
33. Starr, I., Jeffers, W. A. and Meade, R. H. 1943. The absence of conspicuous increments of venous pressure after severe damage to the right ventricle of the dog, with a discussion of the relation between clinical congestive failure and heart disease. *Am. Heart J.* **26**: 291–301. [CrossRef]
34. Suzuki, R., Matsumoto, H., Teshima, T. and Koyama, H. 2013. Clinical assessment of systolic myocardial deformations in dogs with chronic mitral valve insufficiency using two-dimensional speckle-tracking echocardiography. *J. Vet. Cardiol.* **15**: 41–49. [Medline] [CrossRef]
35. Suzuki, R., Matsumoto, H., Teshima, T. and Koyama, H. 2013. Influence of heart rate on myocardial function using two-dimensional speckle-tracking echocardiography in healthy dogs. *J. Vet. Cardiol.* **15**: 139–146. [Medline] [CrossRef]
36. Suzuki, R., Matsumoto, H., Teshima, T. and Koyama, H. 2013. Effect of age on myocardial function assessed by two-dimensional speckle-tracking echocardiography in healthy beagle dogs. *J. Vet. Cardiol.* **15**: 243–252. [Medline] [CrossRef]
37. Tei, C., Ling, L. H., Hodge, D. O., Bailey, K. R., Oh, J. K., Rodeheffer, R. J., Tajik, A. J. and Seward, J. B. 1995. New index of combined systolic and diastolic myocardial performance: a simple and reproducible measure of cardiac function-a study in normals and dilated cardiomyopathy. *J. Cardiol.* **26**: 357–366. [Medline]
38. Teshima, K., Asano, K., Sasaki, Y., Kato, Y., Kutara, K., Edamura, K., Hasegawa, A. and Tanaka, S. 2005. Assessment of left ventricular function using pulsed tissue Doppler imaging in healthy dogs and dogs with spontaneous mitral regurgitation. *J. Vet. Med. Sci.* **67**: 1207–1215. [Medline] [CrossRef]
39. Tidholm, A., Höglund, K., Häggström, J. and Ljungvall, I. 2015. Diagnostic value of selected echocardiographic variables to identify pulmonary hypertension in dogs with myxomatous mitral valve disease. *J. Vet. Intern. Med.* **29**: 1510–1517. [Medline] [CrossRef]
40. Vezzosi, T., Domenech, O., Iacona, M., Marchesotti, F., Zini, E., Venco, L. and Tognetti, R. 2018. Echocardiographic evaluation of the right atrial area index in dogs with pulmonary hypertension. *J. Vet. Intern. Med.* **32**: 42–47. [Medline] [CrossRef]
41. Vezzosi, T., Domenech, O., Costa, G., Marchesotti, F., Venco, L., Zini, E., Del Palacio, M. J. F. and Tognetti, R. 2018. Echocardiographic evaluation of the right ventricular dimension and systolic function in dogs with pulmonary hypertension. *J. Vet. Intern. Med.* **32**: 1541–1548. [Medline] [CrossRef]
42. Vientós-Plotts, A. I., Wiggen, K. E., Lisciandro, G. R. and Reinero, C. R. 2019. The utility of point-of-care ultrasound right-sided cardiac markers as a screening test for moderate to severe pulmonary hypertension in dogs. *Vet. J.* **250**: 6–13. [Medline] [CrossRef]
43. Visser, L. C., Im, M. K., Johnson, L. R. and Stern, J. A. 2016. Diagnostic value of right pulmonary artery distensibility index in dogs with pulmonary hypertension: comparison with doppler echocardiographic estimates of pulmonary arterial pressure. *J. Vet. Intern. Med.* **30**: 543–552. [Medline] [CrossRef]
44. Visser, L. C., Scansen, B. A., Schober, K. E. and Bonagura, J. D. 2015. Echocardiographic assessment of right ventricular systolic function in conscious healthy dogs: repeatability and reference intervals. *J. Vet. Cardiol.* **17**: 83–96. [Medline] [CrossRef]
45. Visser, L. C., Wood, J. E. and Johnson, L. R. 2020. Survival characteristics and prognostic importance of echocardiographic measurements of right heart size and function in dogs with pulmonary hypertension. *J. Vet. Intern. Med.* **34**: 1379–1388. [Medline] [CrossRef]
46. Vonk-Noordegraaf, A., Haddad, F., Chin, K. M., Forfia, P. R., Kawut, S. M., Lumens, J., Naeije, R., Newman, J., Oudiz, R. J., Provencher, S., Torbicki, A., Voelkel, N. F. and Hassoun, P. M. 2013. Right heart adaptation to pulmonary arterial hypertension: physiology and pathobiology. *J. Am. Coll. Cardiol.* **62** Suppl: D22–D33. [Medline] [CrossRef]
47. Wang, Y., Ma, C., Zhang, Y., Guan, Z., Liu, S., Li, Y. and Yang, J. 2015. Assessment of left and right ventricular diastolic and systolic functions using two-dimensional speckle-tracking echocardiography in patients with coronary slow-flow phenomenon. *PLoS One* **10**: e0117979. [Medline] [CrossRef]
48. Yuchi, Y., Suzuki, R., Teshima, T., Matsumoto, H. and Koyama, H. 2021. Utility of tricuspid annular plane systolic excursion normalized by right ventricular size indices in dogs with postcapillary pulmonary hypertension. *J. Vet. Intern. Med.* **35**: 107–119. [Medline] [CrossRef]